
Registers Matter for Pixel-Space Diffusion Transformers

Nikita Starodubcev Ilya Sudakov* Ilya Drobyshevskiy*
Artem Babenko Dmitry Baranchuk

Yandex Research

Abstract

Vision Transformers (ViTs) are known to exhibit high-norm patch-token outliers that degrade feature map quality, a problem effectively mitigated by *register tokens*. As diffusion models increasingly adopt transformer architectures and move toward pixel-space training, they become closer in form to ViTs, raising the question of whether register tokens are also useful for Diffusion Transformers (DiTs). In this work, we show that DiTs differ from ViTs in a key respect: they do not exhibit patch-token outliers. Interestingly, register tokens significantly improve convergence and generation quality of pixel-space DiTs. By analyzing intermediate representations, we find that register tokens produce cleaner feature maps at high noise levels, which may contribute to their effectiveness in pixel-space generation. We further observe that recent pixel-space DiT architectures implicitly incorporate register-like mechanisms, which may partially account for their strong empirical performance. Motivated by these insights, we investigate a parameter-efficient dual-stream architecture that specializes processing for register tokens and improves pixel-space generation quality with negligible runtime overhead.

1 Introduction

Vision Transformers (ViTs) [1, 2, 3] have become a dominant architecture for visual representation learning by modeling images as sequences of patch tokens processed via self-attention [4]. Recent advances in self-supervised learning (SSL) [5, 6, 7] demonstrate that ViTs trained on unlabeled data can learn semantically meaningful representations, enabling object- and part-level understanding useful for downstream tasks such as unsupervised segmentation and detection [8, 9, 10, 6, 11].

Recent research has focused on understanding the emergence of high-norm tokens in ViTs, which are often associated with artifacts in attention maps [12, 13, 14, 15, 16, 17]. As these artifacts lead to less interpretable attention maps and weaker performance on dense prediction tasks, [12] proposes using additional *register tokens* to prevent patch tokens from being repurposed for global representations.

In parallel, diffusion models (DMs) [18, 19] have widely adopted transformer-based architectures [20, 21], replacing convolutional backbones [22, 23]. Recent work has also revisited training directly in pixel space [24, 25, 26], as an alternative to latent diffusion models that rely on pretrained autoencoders [27, 28]. This progress brings Diffusion Transformers (DiTs) closer to ViTs and motivates two questions: (1) *do DiTs inherit high-norm patch-token outliers similar to those observed in ViTs?* and (2) *can register tokens also be effective in these models?*

These questions are also related to broader studies of attention sinks and special-token behavior in transformers [29], including generative models [30, 31, 32, 33, 34]. We defer a detailed discussion of this direction to App. A and focus here on image diffusion transformers, where the presence and role of register-like tokens remain underexplored.

*Equal contribution.

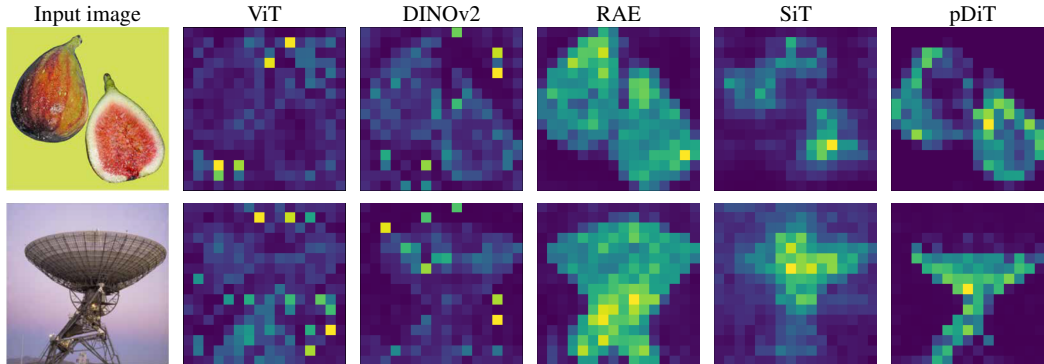


Figure 1: **Diffusion transformers do not exhibit attention-map outliers.** Unlike ViTs, where attention-map anomalies typically appear in low-information regions (e.g., background), DiT attention remains focused on the main objects.

Contributions. We find that, unlike ViTs, diffusion transformers in both latent and pixel spaces do not exhibit noticeable high-norm outliers among patch tokens. Instead, patch-token norms remain relatively uniform, and attention maps lack the low-information artifacts commonly observed in ViTs. Interestingly, despite the absence of such outliers, adding register tokens to DiTs leads to the emergence of high-norm tokens within the registers themselves.

Importantly, we observe that the impact of register tokens differs across training spaces: pixel-space models benefit the most, whereas latent-space models show only moderate gains or even slightly degraded performance.

Accordingly, we focus our study on pixel-space DiTs and find that registers benefit them through mechanisms distinct from those in ViTs. Our analysis shows that registers consistently reduce patch-token feature norms and produce smoother intermediate feature maps, especially at high noise levels. Moreover, register tokens specialize into distinct roles: some act as norm sinks, while others encode global semantic information.

These findings also provide a rationale for recent pixel-space DiT designs [24, 26], which introduce additional in-context class-conditioning and achieve substantial performance gains. Our analysis suggests that these gains may largely arise from register-like behavior rather than from additional class information. In particular, in-context tokens behave similarly to register tokens, with some encoding global semantic information and others acting as norm sinks.

Finally, we explore a parameter-efficient dual-stream architecture that processes register and patch tokens as distinct streams while sharing attention and most transformer parameters. This specialization improves generation quality at similar inference cost, with only a $\sim 14\%$ increase in model size.

2 Register Tokens for Image Diffusion Transformers

In this section, we analyze the role of register tokens in DiTs and highlight key differences from their use in ViTs. As a representative ViT-based model, we consider DINOv2 [6].

For diffusion models, we primarily focus on pixel-space DiTs based on the standard architecture [20] with widely used transformer improvements [35, 24]; we refer to these models as pDiTs. We train pDiTs using flow matching [36, 37] on ImageNet [38] at resolution 256×256 with patch size 16. We additionally analyze latent-space architectures, SiT [21] and RAE [39], using their original backbone designs and training pipelines. For RAE, we use a DINOv2-based model [6]. Generation quality is evaluated using FID [40].

We study models of varying sizes, with and without register tokens. Registers are implemented as additional learnable tokens appended to the patch-token sequence following [12] and are not used in the training objective. Further details are provided in App. B.

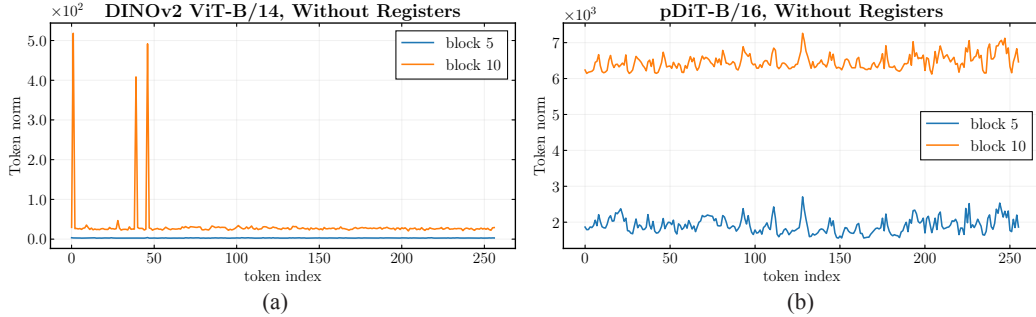


Figure 2: **Without Registers.** (a) In DINOv2, anomalies are localized to few image tokens, which exhibit significantly higher norms than others. (b) In contrast, no outliers are observed for pDiTs, suggesting that registers may be unnecessary in this case.

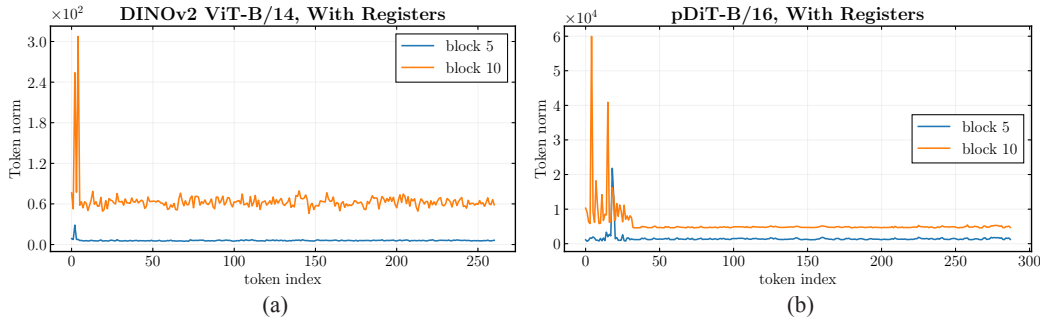


Figure 3: **With Registers.** (a) As expected, introducing register tokens in DINOv2 shifts high-norm outliers into these tokens. (b) Interestingly, pDiTs also exhibit high-norm tokens in the added registers, even though such outliers are absent without registers.

Epoch	pDiT-B/16, 131M			pDiT-L/16, 459M			pDiT-H/16, 953M		
	w/o reg.	w/ reg.	w/ in-context	w/o reg.	w/ reg.	w/ in-context	w/o reg.	w/ reg.	w/ in-context
200	7.39	5.30	4.71	4.13	3.17	2.95	3.31	2.61	2.51
600	4.80	3.80	3.71	2.80	2.47	2.43	2.62	2.35	2.23

Table 1: **Generation quality (FID) of pDiTs w/ and w/o register tokens.** Models with registers consistently outperform those without registers across model sizes and training epochs on ImageNet 256×256 . The shaded column reports performance with in-context class conditioning (Section 2.6).

2.1 Registers Benefit Diffusion Transformers Despite the Absence of Outliers

The motivation for introducing register tokens in ViTs is to mitigate outliers in feature maps. These outliers manifest as high-norm tokens, often localized in low-information regions, e.g., background.

We first investigate whether such outliers arise in DiTs without registers for different spaces by comparing their attention maps to those of ViTs. As shown in Figure 1, DiTs do not exhibit the artifacts observed in ViTs. In particular, their attention maps remain free of anomalies in low-information regions, which in ViTs are typically associated with unusually high-norm tokens.

This observation is further supported by Figure 2, which reports token-wise feature norms across layers for pDiT. In contrast to DINOv2, where a few tokens attain significantly larger norms, pDiTs exhibit a nearly uniform distribution of patch-token norms. As shown in Figure 10, 11 this behavior consistently holds across larger model variants and latent-space architectures.

Based on these observations, DiTs would not be expected to benefit from register tokens, as the feature map artifacts that originally motivated their use are absent. However, contrary to this expectation, we observe the opposite.

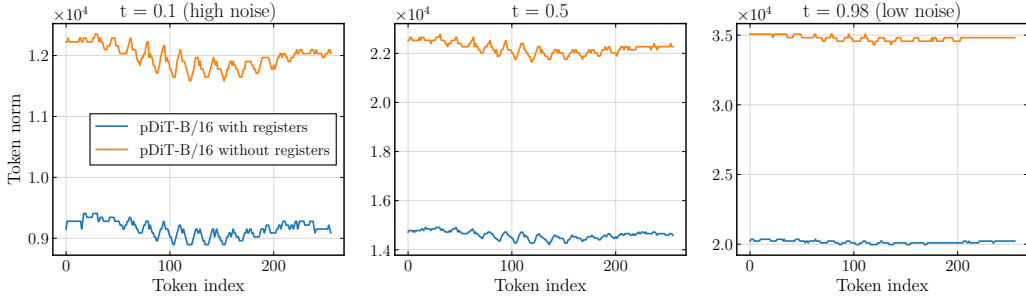


Figure 4: **Register tokens consistently reduce feature norms across patch tokens.** We measure feature norms for image tokens only (excluding registers) at three diffusion timesteps and observe a consistent reduction across all tokens when registers are used.

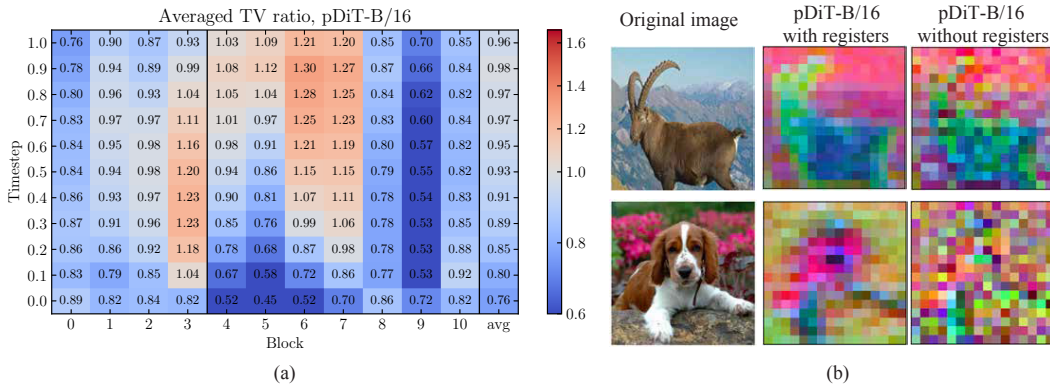


Figure 5: **Register tokens improve intermediate representations.** (a) We compute the Total Variation (TV) of intermediate features for models with and without register tokens. We report the ratio (with / without registers), where lower values indicate that the model with registers produces smoother features. We find that registers improve feature smoothness at high noise levels ($t \in [0, 0.2]$). (b) We visualize feature maps using PCA, which qualitatively confirms this effect.

First, in Figure 3, we compare token-wise feature norms for DINOv2 and pDiTs with register tokens. As expected, in DINOv2, registers primarily absorb pre-existing outliers from patch tokens. In contrast, pDiTs develop high-norm tokens within the registers, despite the absence of such outliers in models without registers. Figures 9, 10, 11 show that it consistently holds across different timesteps and extends to latent-space models as well.

Second, as shown in Table 1, introducing register tokens in pDiTs leads to consistent improvements in generation quality across model sizes. However, Table 2 shows that registers provide significantly smaller gains in latent-space models, a phenomenon we discuss in Section 2.4.

Based on these observations, pDiTs benefit from the presence of outliers but lack a mechanism to accommodate them in the absence of register tokens. We attribute this to all patch tokens in DiTs contributing to the loss, leaving no capacity for specialized outlier tokens. In contrast, in ViTs, only a few tokens participate in the loss, allowing high-norm outliers to emerge among image tokens. When register tokens are introduced, they similarly do not participate in the loss, thereby providing convenient slots for such high-norm outliers.

2.2 Register Tokens Lead to Cleaner Internal Feature Maps

The previous analysis shows that register tokens significantly improve pDiT performance, but their functional role remains unclear. In particular, their effect differs from that in ViTs, where registers primarily absorb pre-existing outliers. We therefore investigate how registers influence the internal representations of diffusion models, focusing on pixel-space models where their impact is strongest.

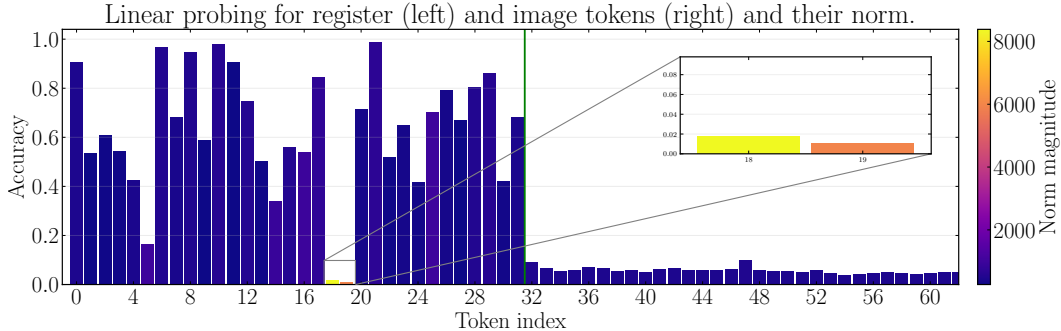


Figure 6: **Register tokens act as both global information carriers and norm sinks.** Linear probing reveals that low-norm register tokens encode meaningful global semantics and achieve strong classification accuracy, whereas low-accuracy registers exhibit extremely large norms, suggesting that they primarily function as norm sinks that absorb magnitude from patch tokens.

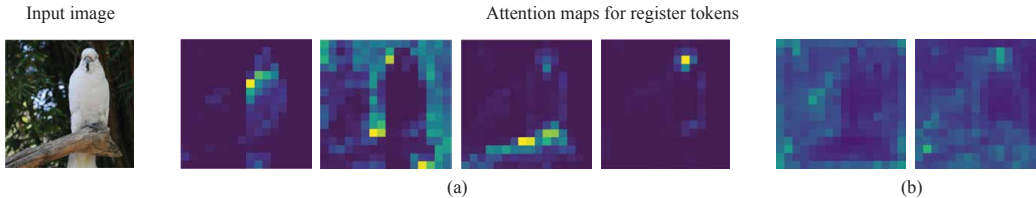


Figure 7: **(a) Registers with high probing accuracy encode diverse semantic information about an image, whereas (b) low-accuracy norm sinks do not.** We visualize attention maps for register tokens and observe that some attend to distinct semantic regions, such as foreground objects and background areas. In contrast, norm sinks with low probing accuracy do not exhibit meaningful semantic structure.

First, we find that register tokens influence all image tokens by consistently reducing their feature norms (Figure 4). Interestingly, DINOv2 register tokens do not exhibit this behavior for non-outlier patch tokens (see Figure 19).

A possible explanation for this behavior is that larger feature norms may reflect high local variability in hidden representations. In diffusion models, such variability may arise from the models’ need to carefully predict high-dimensional targets, causing all information, including global semantics and low-level signals, to propagate through patch tokens. Register tokens may absorb part of this information, reducing patch-token norms and allowing patch tokens to form smoother, more spatially structured representations.

To examine this, we consider Total Variation (TV) [41], which measures spatial smoothness by quantifying intensity differences between adjacent pixels. In our case, we use TV to quantify the spatial smoothness of intermediate transformer features. Specifically, we extract feature maps after each transformer block at different diffusion timesteps and compute their TV averaged over 1K images. We then evaluate TV value ratios (with registers / without registers).

We present the results in Figure 5(a) and observe that the ratios remain below 1 at lower timesteps (noisier images) and gradually approach 1 at higher timesteps (less noisy images). This suggests that register tokens improve feature smoothness primarily at high-noise levels ($t \in [0, 0.2]$). Figure 5(b) provides qualitative support for this observation: PCA visualizations of intermediate features at $t = 0.1$ show that models with registers produce smoother and more coherent feature representations.

Note that high-noise levels are particularly important for flow-matching models in high-dimensional spaces [42, 43], as they play a central role in forming the main image content. Therefore, the improved representations induced by register tokens at these stages provide a plausible explanation for the observed quality gains.

	RAE-space DiT ^{DB} backbone	VAE-space SiT backbone	Pixel-space pDiT backbone
<i>Base size</i>			
w/ reg.	7.48	9.40	5.30
w/o reg.	6.58	10.40	7.39
<i>Large size</i>			
w/ reg.	4.44	2.38	2.61
w/o reg.	3.91	2.53	3.31

Table 2: **Registers are more effective in pixel-space.** Generation quality for models with and without registers across different training spaces and model sizes. Registers yield the largest improvements in pixel space, moderate gains in VAE space, and degraded performance in RAE space.

	Registers configuration			FID at Epoch		
	Size	Start	End	40	80	120
w/ reg.	32	4	11	37.7	9.59	6.45
	32	4	9	36.9	9.95	6.65
	32	0	11	59.7	19.3	11.9
	32	0	4	62.4	19.6	12.3
	16	4	11	40.4	10.2	6.80
	4	4	11	46.3	12.8	8.37
w/o reg.	—	—	—	60.6	18.4	11.1

Table 3: **Registers are effective only in deeper layers.** Unlike DINOv2, pDiT-B/16 benefits from register tokens only when they are introduced after the first 4 layers. Increasing the number of registers further improves performance.

2.3 Registers Do Both: Encode Global Information and Act as Norm Sinks

Next, we find that, beyond acting as norm sinks for patch tokens, register tokens can encode diverse global information about the input image. Specifically, we perform linear probing using register-token features extracted from an intermediate transformer block (the 5th out of 12 blocks).

Figure 6 shows that classification accuracy is highly diverse: some tokens achieve high accuracy (≈ 0.9), others moderate (≈ 0.4), and some very low (≈ 0.02). These results suggest the following: (a) tokens with the highest norms act as norm sinks, yielding the lowest accuracy; (b) tokens with moderate norms encode diverse information about the image beyond class-specific features.

To further validate that non-sink tokens encode diverse information, we visualize attention maps of different register tokens (Figure 7a). We observe that registers attend to distinct semantic regions of the image. In the example, some tokens focus on background elements (e.g., jungle), while others attend to object parts (e.g., bird, branch, beak). In contrast, norm sinks do not encode meaningful semantic information (Figure 7b).

Discussion. The insights from Sections 2.2 and 2.3 may relate to recent representation-alignment methods [44, 45], which improve DM convergence by aligning diffusion internal representations with vision encoders, e.g., DINOv2. Notably, iREPA [45] shows that generation quality benefits more from aligning spatial structure than global semantics. This aligns with our analysis: register tokens absorb global semantic information while improving the spatial coherence of patch tokens, suggesting that registers may play a regularizing role similar to REPA. We therefore explore whether register tokens complement REPA-like objectives in App. D.

2.4 Registers Are More Effective in Pixel Space

In Table 2, we compare the models operating in different spaces with and without registers. We find that register tokens show the largest improvements in pixel space, provide smaller gains in VAE space [39], and, interestingly, degrade performance in RAE-based models [39].

To isolate the effect of different diffusion backbones, we apply the pDiT backbone to RAE and VAE spaces as well. The results presented in Table 8 show the same trend. This indicates that the effect of register tokens is not related to corresponding architectural differences.

To better understand this effect, we analyze the smoothness of intermediate representations in DiTs without registers using TV. As shown in Figure 18, pixel-space models produce the least smooth (i.e., noisiest) intermediate features compared to latent DMs. In addition, we find that pixel-space models exhibit the highest feature norms for all patch tokens, further supporting this observation.

These findings further suggest that training DMs in pixel space is inherently more challenging and requires stronger regularization. In contrast, latent spaces are more structured and lower-dimensional, where imperceptible noise and fine-grained details are compressed. As a result, register tokens appear less critical for latent-space models, while serving as an effective mechanism for improving degraded representations in pixel-space DiTs.

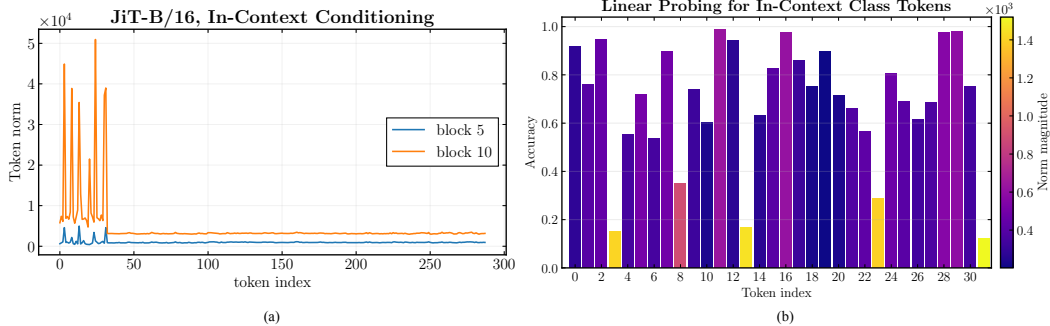


Figure 8: **In-context class tokens act as registers.** (a) Certain tokens acquire disproportionately high feature norms, functioning as norm sinks. (b) Some tokens encode broad global information, rather than purely class-specific features as originally intended.

2.5 Registers Are Effective in Deeper Layers

Next, we ablate both the number of register tokens and the transformer blocks in which they are introduced. We consider pDiT-B with 12 layers. Based on the results in Table 3, we observe two key differences compared to standard ViTs. We explore additional configurations in Table 10.

First, pDiTs benefit from enabling register tokens only in deeper blocks (4–11), whereas ViTs use them from the first layer [12]. For example, applying registers throughout all layers (0–11) provides performance comparable to the model without registers. A similar effect appears for early-layer registers (0–4). Moreover, the 4–9 configuration suggests that the final layers contribute less.

Previously, we found that register tokens encode diverse semantic information about the input image and help form more structured representations. We hypothesize that their ineffectiveness in early layers stems from the lack of semantic structure at this stage. Specifically, early-layer registers primarily capture low-level or non-informative signals, providing weak conditioning to subsequent layers and ultimately degrading performance. To support this observation, Figure 16 compares linear probing results for models with register tokens introduced at layers 4 and 0. When registers are enabled from the beginning, many non-sink registers capture little semantic information after the 5th block, resulting in weak signals that are subsequently propagated to further layers.

Second, we observe that pDiTs require more register tokens than ViTs. While 4 registers are typically sufficient for ViTs [12, 7], pDiT-B achieves the best performance with 32 registers. This suggests that registers in DiTs are required to solve a more challenging task, necessitating a larger number of tokens.

2.6 Registers Are Implicitly Present in Existing Diffusion Transformers

Recent DiTs incorporate conditioning signals (e.g., text or class labels) by appending additional tokens to the sequence of image patches and processing them jointly through shared transformer layers. For example, JiT [24], a pixel-space DiT, employs in-context conditioning by adding duplicated class embeddings to the input sequence, leading to notable improvements in generation quality. This raises the question of whether such in-context tokens implicitly function as register tokens.

To address this, we train JiT-B/16 with in-context conditioning, using the same diffusion backbone and number of tokens as in the register setting. Thus, the only difference between JiT-B/16 and pDiT-B/16 lies in the additional token sequence (in-context vs register tokens).

Then, we measure the norms of in-context tokens (Figure 8a) and evaluate their representations using linear probing (Figure 8b). Interestingly, we observe similar behavior as for registers: (a) some tokens encode diverse global information rather than only class-specific features as originally intended, (b) while others act as norm sinks. This suggests that in-context tokens implicitly behave as registers.

Moreover, Table 1 compares models with registers, without registers, and with in-context conditioning. We find that most of the improvement over the baseline comes from the presence of pure register tokens rather than from the additional class information itself, helping explain the large quality

gains from in-context conditioning. However, in-context conditioning further improves performance, suggesting that such tokens help the model form better initial representations.

We note that JiT [24] introduces in-context tokens only in deeper layers, which motivates our ablation study on the register starting layer in Section 2.5.

We also analyze large-scale text-to-image models based on MM-DiT [42], where text tokens are appended to image tokens. Interestingly, we observe a similar phenomenon: some text tokens exhibit high-norm outlier behavior (Figure 20), suggesting they may act as implicit registers.

3 Decoupled Processing of Register and Patch Tokens

Dual-stream architecture. Our analysis reveals that register and patch tokens play distinct roles, yet existing pixel-space architectures [24, 26] process them identically using fully shared parameters. Given their differing behaviors, such parameter sharing may be suboptimal.

In contrast, large-scale models with appended auxiliary sequences (e.g., text tokens) often employ dual-stream architectures [42, 46], where separate parameters are used for different token types while interactions are maintained through attention. Motivated by these differences, we investigate dual-stream designs that enable specialized processing of register tokens in pixel-space DiTs.

We consider the JiT architecture [24], which uses in-context conditioning. JiT blocks consist of RMSNorm, adaLN, Attention, and MLP layers. Thus, we selectively introduce token-specific specialization in these components.

In Table 4, we evaluate naive dual-stream designs that separately duplicate transformer components for register and patch tokens. Duplicating all components gives the best performance but significantly increases parameters. Among individual components, adaLN and MLP contribute the most, while Attention and RMSNorm provide limited gains.

Compact dual-stream design. As we find, naive duplication leads to a significant increase in parameters. We therefore explore parameter-efficient strategies for selective duplication.

For RMSNorm, which has few parameters, we use separate parameters for register and patch tokens with negligible cost (Snippet 1).

For parameter-intensive modules (adaLN, Attention, and MLP), we avoid full duplication. In MLP, we compute a shared SwiGLU (Linear projection followed by SiLU gating) and apply separate output projections for register and patch tokens (Snippet 2).

For adaLN and Attention, we use parameter-efficient LoRA adaptations [47], following [48]. Shared parameters are computed for all tokens, while lightweight LoRA branches are applied only to register tokens. In adaLN, normalization parameters are first shared across all tokens, then refined for register tokens via a LoRA branch (Snippet 3). In Attention, QKV projections are shared, with LoRA applied only to register-token representations, while the output projection remains shared.

Our final architecture combines single-stream and dual-stream transformer layers. Motivated by the ablation results in Table 3, which show that register tokens are ineffective in early layers, we first process the image sequence using standard single-stream layers. Register tokens are then introduced only in later stages, where the model transitions to dual-stream processing. The overall design increases the parameter count by only $\sim 14\%$, compared to $\sim 77\%$ for naive duplication.

Results. We first study which components should be decoupled in the compact dual-stream design. We use JiT-B/16 adapted to a dual-stream architecture and train it on ImageNet 256×256 for 600 epochs, following the training and sampling setups of [24]. We enable in-context tokens at layer 4, resulting in single-stream layers 0–3 and dual-stream layers 4–11.

Table 5 reports the results for several parameter-efficient dual-stream designs, compared against the single-stream JiT-B/16 baseline (gray-shaded row).

Applying the dual architecture to all layers improves FID from 3.71 to 3.48. Sharing Attention further improves performance while reducing parameters, suggesting that attention decoupling is unnecessary. In contrast, sharing MLP significantly degrades performance, while removing dual adaLN or RMSNorm also hurts results. Based on these findings, our final compact design dualizes MLP, adaLN, and RMSNorm, while keeping Attention shared (green-shaded row).

adaLN	MLP	Attn	RMSNorm	Params (M)	FID
				131M	3.71
✓	✓	✓	✓	230M	3.14
✓				173M	3.44
	✓			168M	3.44
		✓		150M	3.61
			✓	131M	3.70

Table 4: **Ablation of dual-stream designs.** We separately duplicate transformer components for register and patch tokens. Duplicating all components gives the best performance but significantly increases parameters. Among individual components, adaLN and MLP contribute the most, while Attention and RMSNorm provide limited gains. gray denotes the single-stream JiT-B/16 baseline.

Model	Params (M)	GFLOPs	Epoch	FID
JiT-B/16	131	23.8	200 600	4.71 3.71
JiT-L/16	459	84.2	200 600	2.95 2.43
Ours-B/16	149	23.8	200 600	4.25 3.41
Ours-L/16	518	84.2	200 600	2.76 2.32

Table 6: Comparison of our compact dual-stream architecture with the JiT baseline on ImageNet 256×256 .

adaLN	MLP	Attn	RMSNorm	Params (M)	FID
				131M	3.71
✓	✓	✓	✓	161M	3.48
✓	✓		✓	149M	3.41
✓			✓	136M	3.81
	✓		✓	143M	3.56
✓	✓			149M	3.53

Table 5: **Ablation of compact dual-stream designs.** We evaluate parameter-efficient dual-stream configurations by selectively dualizing transformer components for register and patch tokens. The best compact design (green) dualizes adaLN, MLP, and RMSNorm, while keeping Attention shared, achieving the best trade-off between parameter count and generation quality.

Model	Params (M)	GFLOPs	Epoch	FID
JiT-B/32	133	24.3	200 600	5.84 4.12
JiT-L/32	461	84.8	200 600	3.28 2.69
Ours-B/32	151	24.3	200 600	4.98 3.92
Ours-L/32	520	84.8	200 600	3.08 2.57

Table 7: Comparison of our compact dual-stream architecture with the JiT baseline on ImageNet 512×512 .

Next, we conduct a system-level comparison between our compact dual architecture and the JiT baseline on ImageNet 256×256 and 512×512 across different model sizes. For all variants, we follow the training setup and baseline configurations of [24].

We report the results in Tables 6 and 7. The parameter-efficient dual-stream architecture consistently improves generation quality across model scales and image resolutions, while introducing only a small increase in parameters and no additional runtime overhead in terms of GFLOPs.

We believe our compact strategy can provide greater benefits at larger scales, where dual-stream architectures [42] achieve significant quality improvements. In these settings, the appended sequence, e.g., text, becomes substantially larger than the small set of register tokens.

4 Discussion

This work presents a systematic study of register tokens in image DiTs. We show that registers exhibit behavior distinct from patch tokens and play a particularly important role in pixel-space models, where they promote cleaner and more structured intermediate representations. Motivated by these findings, we explore register-aware architectural designs and demonstrate that specialized processing of register tokens can improve generation quality with negligible runtime overhead.

At the same time, we believe the proposed designs only partially capture the promise of token specialization. This suggests that the question of how to effectively utilize registers in pixel-space diffusion transformers remains open. We hope that our findings provide a useful step in this direction and motivate future work on methods that more fully exploit this potential.

References

- [1] Alexey Dosovitskiy, Lucas Beyer, Alexander Kolesnikov, Dirk Weissenborn, Xiaohua Zhai, Thomas Unterthiner, Mostafa Dehghani, Matthias Minderer, Georg Heigold, Sylvain Gelly, et al. An image is worth 16x16 words: Transformers for image recognition at scale. *arXiv preprint arXiv:2010.11929*, 2020.
- [2] Ze Liu, Yutong Lin, Yue Cao, Han Hu, Yixuan Wei, Zheng Zhang, Stephen Lin, and Baining Guo. Swin transformer: Hierarchical vision transformer using shifted windows. In *Proceedings of the IEEE/CVF international conference on computer vision*, pages 10012–10022, 2021.
- [3] Hugo Touvron, Matthieu Cord, Matthijs Douze, Francisco Massa, Alexandre Sablayrolles, and Hervé Jégou. Training data-efficient image transformers & distillation through attention. In *International conference on machine learning*, pages 10347–10357. PMLR, 2021.
- [4] Ashish Vaswani, Noam Shazeer, Niki Parmar, Jakob Uszkoreit, Llion Jones, Aidan N Gomez, Łukasz Kaiser, and Illia Polosukhin. Attention is all you need. *Advances in neural information processing systems*, 30, 2017.
- [5] Mathilde Caron, Hugo Touvron, Ishan Misra, Hervé Jégou, Julien Mairal, Piotr Bojanowski, and Armand Joulin. Emerging properties in self-supervised vision transformers. In *Proceedings of the IEEE/CVF international conference on computer vision*, pages 9650–9660, 2021.
- [6] Maxime Oquab, Timothée Darcet, Théo Moutakanni, Huy Vo, Marc Szafraniec, Vasil Khalidov, Pierre Fernandez, Daniel Haziza, Francisco Massa, Alaaeldin El-Nouby, et al. Dinov2: Learning robust visual features without supervision. *arXiv preprint arXiv:2304.07193*, 2023.
- [7] Oriane Siméoni, Huy V Vo, Maximilian Seitzer, Federico Baldassarre, Maxime Oquab, Cijo Jose, Vasil Khalidov, Marc Szafraniec, Seungeun Yi, Michaël Ramamonjisoa, et al. Dinov3. *arXiv preprint arXiv:2508.10104*, 2025.
- [8] Oriane Siméoni, Gilles Puy, Huy V Vo, Simon Roburin, Spyros Gidaris, Andrei Bursuc, Patrick Pérez, Renaud Marlet, and Jean Ponce. Localizing objects with self-supervised transformers and no labels. *arXiv preprint arXiv:2109.14279*, 2021.
- [9] Mark Hamilton, Zhoutong Zhang, Bharath Hariharan, Noah Snavely, and William T Freeman. Unsupervised semantic segmentation by distilling feature correspondences. *arXiv preprint arXiv:2203.08414*, 2022.
- [10] Shir Amir, Yossi Gandelsman, Shai Bagon, and Tali Dekel. Deep vit features as dense visual descriptors. *arXiv preprint arXiv:2112.05814*, 2(3):4, 2021.
- [11] Yangtao Wang, Xi Shen, Yuan Yuan, Yuming Du, Maomao Li, Shell Xu Hu, James L Crowley, and Dominique Vaufreydaz. Tokencut: Segmenting objects in images and videos with self-supervised transformer and normalized cut. *IEEE transactions on pattern analysis and machine intelligence*, 45(12):15790–15801, 2023.
- [12] Timothée Darcet, Maxime Oquab, Julien Mairal, and Piotr Bojanowski. Vision transformers need registers. *arXiv preprint arXiv:2309.16588*, 2023.
- [13] Nick Jiang, Amil Dravid, Alexei Efros, and Yossi Gandelsman. Vision transformers don’t need trained registers. *arXiv preprint arXiv:2506.08010*, 2025.
- [14] Alexander Lappe and Martin A Giese. Register and [cls] tokens induce a decoupling of local and global features in large vits. In *The Thirty-ninth Annual Conference on Neural Information Processing Systems*, 2025.
- [15] Cheng Shi, Yizhou Yu, and Sibeï Yang. Vision transformers need more than registers. *arXiv preprint arXiv:2602.22394*, 2026.
- [16] Yinjie Chen, Zipeng Yan, Chong Zhou, Bo Dai, and Andrew F Luo. Vision transformers with self-distilled registers. *arXiv preprint arXiv:2505.21501*, 2025.
- [17] Haoqi Wang, Tong Zhang, and Mathieu Salzmann. Sinder: Repairing the singular defects of dinov2. In *European Conference on Computer Vision*, pages 20–35. Springer, 2024.

- [18] Jonathan Ho, Ajay Jain, and Pieter Abbeel. Denoising diffusion probabilistic models. *Advances in neural information processing systems*, 33:6840–6851, 2020.
- [19] Yang Song and Stefano Ermon. Generative modeling by estimating gradients of the data distribution. *Advances in neural information processing systems*, 32, 2019.
- [20] William Peebles and Saining Xie. Scalable diffusion models with transformers. In *Proceedings of the IEEE/CVF international conference on computer vision*, pages 4195–4205, 2023.
- [21] Nanye Ma, Mark Goldstein, Michael S Albergo, Nicholas M Boffi, Eric Vanden-Eijnden, and Saining Xie. Sit: Exploring flow and diffusion-based generative models with scalable interpolant transformers. In *European Conference on Computer Vision*, pages 23–40. Springer, 2024.
- [22] Olaf Ronneberger, Philipp Fischer, and Thomas Brox. U-net: Convolutional networks for biomedical image segmentation. In *International Conference on Medical image computing and computer-assisted intervention*, pages 234–241. Springer, 2015.
- [23] Prafulla Dhariwal and Alexander Nichol. Diffusion models beat gans on image synthesis. *Advances in neural information processing systems*, 34:8780–8794, 2021.
- [24] Tianhong Li and Kaiming He. Back to basics: Let denoising generative models denoise. *arXiv preprint arXiv:2511.13720*, 2025.
- [25] Yongsheng Yu, Wei Xiong, Weili Nie, Yichen Sheng, Shiqiu Liu, and Jiebo Luo. Pixeldit: Pixel diffusion transformers for image generation. *arXiv preprint arXiv:2511.20645*, 2025.
- [26] Yiyang Lu, Susie Lu, Qiao Sun, Hanhong Zhao, Zhicheng Jiang, Xianbang Wang, Tianhong Li, Zhengyang Geng, and Kaiming He. One-step latent-free image generation with pixel mean flows. *arXiv preprint arXiv:2601.22158*, 2026.
- [27] Robin Rombach, Andreas Blattmann, Dominik Lorenz, Patrick Esser, and Björn Ommer. High-resolution image synthesis with latent diffusion models. In *Proceedings of the IEEE/CVF conference on computer vision and pattern recognition*, pages 10684–10695, 2022.
- [28] Dustin Podell, Zion English, Kyle Lacey, Andreas Blattmann, Tim Dockhorn, Jonas Müller, Joe Penna, and Robin Rombach. Sdxl: Improving latent diffusion models for high-resolution image synthesis. *arXiv preprint arXiv:2307.01952*, 2023.
- [29] Zunhai Su, Hengyuan Zhang, Wei Wu, Yifan Zhang, Yaxiu Liu, He Xiao, Qingyao Yang, Yuxuan Sun, Rui Yang, Chao Zhang, et al. Attention sink in transformers: A survey on utilization, interpretation, and mitigation. *arXiv preprint arXiv:2604.10098*, 2026.
- [30] Guangxuan Xiao, Yuandong Tian, Beidi Chen, Song Han, and Mike Lewis. Efficient streaming language models with attention sinks. *arXiv preprint arXiv:2309.17453*, 2023.
- [31] Xiangming Gu, Tianyu Pang, Chao Du, Qian Liu, Fengzhuo Zhang, Cunxiao Du, Ye Wang, and Min Lin. When attention sink emerges in language models: An empirical view. *arXiv preprint arXiv:2410.10781*, 2024.
- [32] Maximo Eduardo Rulli, Simone Petrucci, Edoardo Michielon, Fabrizio Silvestri, Simone Scardapane, and Alessio Devoto. Attention sinks in diffusion language models. *arXiv preprint arXiv:2510.15731*, 2025.
- [33] Kunhao Liu, Wenbo Hu, Jiale Xu, Ying Shan, and Shijian Lu. Rolling forcing: Autoregressive long video diffusion in real time. *arXiv preprint arXiv:2509.25161*, 2025.
- [34] Amna Jamal, Mika Tan, Clarissa Aurelia Nahid Saputra, Quan Huynh, Kevin Zhu, and Antonio Mari. Diffusion transformers use sink registers. In *Second Workshop on XAI4Science: From Understanding Model Behavior to Discovering New Scientific Knowledge*, 2026.
- [35] Jingfeng Yao, Bin Yang, and Xinggang Wang. Reconstruction vs. generation: Taming optimization dilemma in latent diffusion models. In *Proceedings of the Computer Vision and Pattern Recognition Conference*, pages 15703–15712, 2025.

- [36] Yaron Lipman, Ricky T. Q. Chen, Heli Ben-Hamu, Maximilian Nickel, and Matthew Le. Flow matching for generative modeling. In *The Eleventh International Conference on Learning Representations*, 2023.
- [37] Michael Albergo, Nicholas M Boffi, and Eric Vanden-Eijnden. Stochastic interpolants: A unifying framework for flows and diffusions. *Journal of Machine Learning Research*, 26(209):1–80, 2025.
- [38] Jia Deng, Wei Dong, Richard Socher, Li-Jia Li, Kai Li, and Li Fei-Fei. Imagenet: A large-scale hierarchical image database. In *2009 IEEE conference on computer vision and pattern recognition*, pages 248–255. Ieee, 2009.
- [39] Boyang Zheng, Nanye Ma, Shengbang Tong, and Saining Xie. Diffusion transformers with representation autoencoders. In *The Fourteenth International Conference on Learning Representations*, 2026.
- [40] Martin Heusel, Hubert Ramsauer, Thomas Unterthiner, Bernhard Nessler, and Sepp Hochreiter. Gans trained by a two time-scale update rule converge to a local nash equilibrium. *Advances in neural information processing systems*, 30, 2017.
- [41] Leonid I Rudin, Stanley Osher, and Emad Fatemi. Nonlinear total variation based noise removal algorithms. *Physica D: nonlinear phenomena*, 60(1-4):259–268, 1992.
- [42] Patrick Esser, Sumith Kulal, Andreas Blattmann, Rahim Entezari, Jonas Müller, Harry Saini, Yam Levi, Dominik Lorenz, Axel Sauer, Frederic Boesel, et al. Scaling rectified flow transformers for high-resolution image synthesis. In *Forty-first international conference on machine learning*, 2024.
- [43] Black Forest Labs. FLUX.2: Analyzing and enhancing the latent space of FLUX – representation comparison, 2025.
- [44] Sihyun Yu, Sangkyung Kwak, Huiwon Jang, Jongheon Jeong, Jonathan Huang, Jinwoo Shin, and Saining Xie. Representation alignment for generation: Training diffusion transformers is easier than you think. *arXiv preprint arXiv:2410.06940*, 2024.
- [45] Jaskirat Singh, Xingjian Leng, Zongze Wu, Liang Zheng, Richard Zhang, Eli Shechtman, and Saining Xie. What matters for representation alignment: Global information or spatial structure? *arXiv preprint arXiv:2512.10794*, 2025.
- [46] Black Forest Labs. Flux. <https://github.com/black-forest-labs/flux>, 2024.
- [47] Edward J Hu, Yelong Shen, Phillip Wallis, Zeyuan Allen-Zhu, Yanzhi Li, Shean Wang, Lu Wang, and Weizhu Chen. LoRA: Low-rank adaptation of large language models. In *International Conference on Learning Representations*, 2022.
- [48] Alexis Marouani, Oriane Siméoni, Hervé Jégou, Piotr Bojanowski, and Huy V Vo. Revisiting [cls] and patch token interaction in vision transformers. *arXiv preprint arXiv:2602.08626*, 2026.
- [49] Mingjie Sun, Xinlei Chen, J Zico Kolter, and Zhuang Liu. Massive activations in large language models. *arXiv preprint arXiv:2402.17762*, 2024.
- [50] Itay Yona, Ilia Shumailov, Jamie Hayes, Federico Barbero, and Yossi Gandelsman. Interpreting the repeated token phenomenon in large language models. *arXiv preprint arXiv:2503.08908*, 2025.
- [51] Zihan Qiu, Zekun Wang, Bo Zheng, Zeyu Huang, Kaiyue Wen, Songlin Yang, Rui Men, Le Yu, Fei Huang, Suozhi Huang, et al. Gated attention for large language models: Non-linearity, sparsity, and attention-sink-free. *arXiv preprint arXiv:2505.06708*, 2025.
- [52] Zihou Zhang, Zheyong Xie, Li Zhong, Haifeng Liu, Yao Hu, and Shaosheng Cao. One token is enough: Improving diffusion language models with a sink token. *arXiv preprint arXiv:2601.19657*, 2026.
- [53] Yuxin Wen, Jim Wu, Ajay Jain, Tom Goldstein, and Ashwinee Panda. Analysis of attention in video diffusion transformers. *arXiv preprint arXiv:2504.10317*, 2025.

- [54] Joonghyuk Shin, Zhengqi Li, Richard Zhang, Jun-Yan Zhu, Jaesik Park, Eli Shechtman, and Xun Huang. Motionstream: Real-time video generation with interactive motion controls. *arXiv preprint arXiv:2511.01266*, 2025.
- [55] Jung Yi, Wooseok Jang, Paul Hyunbin Cho, Jisu Nam, Heeji Yoon, and Seungryong Kim. Deep forcing: Training-free long video generation with deep sink and participative compression. *arXiv preprint arXiv:2512.05081*, 2025.
- [56] Mingyang Yi, Aoxue Li, Yi Xin, and Zhenguo Li. Towards understanding the working mechanism of text-to-image diffusion model. *Advances in Neural Information Processing Systems*, 37:55342–55369, 2024.
- [57] Yongqi An, Xu Zhao, Tao Yu, Ming Tang, and Jinqiao Wang. Systematic outliers in large language models. *arXiv preprint arXiv:2502.06415*, 2025.
- [58] Chaofan Gan, Yuanpeng Tu, Xi Chen, Tiejuan Chen, Yuxi Li, Mehrtash Harandi, and Weiyao Lin. Unleashing diffusion transformers for visual correspondence by modulating massive activations. *Advances in Neural Information Processing Systems*, 38:114432–114462, 2026.
- [59] Chaofan Gan, Zicheng Zhao, Yuanpeng Tu, Xi Chen, Ziran Qin, Tiejuan Chen, Mehrtash Harandi, and Weiyao Lin. Massive activations are the key to local detail synthesis in diffusion transformers. *arXiv preprint arXiv:2510.11538*, 2025.
- [60] Jaeyo Shin, Jiwook Kim, and Hyunjung Shim. Representation alignment for just image transformers is not easier than you think. *arXiv preprint arXiv:2603.14366*, 2026.

A Related Work

Attention Sinks in Large Language Models. In autoregressive LLMs, attention sinks are a well-explored area [30, 49, 31, 50, 51]. [30] first analyzes anomalies in attention and finds that a large portion of the attention score is allocated to the initial tokens, making them attention sinks. The authors propose preserving these initial register tokens during inference, which leads to a significant quality boost. [49] continues the sink analysis and finds that outliers appear in a few fixed feature dimensions, regardless of the input, as well as in two types of special tokens. [31] analyzes why and how attention sinks emerge during training. [50] explores the functional role of attention sinks, showing their connection to the repeated token divergence phenomenon. [51] demonstrates that sparse gating can eliminate attention sinks.

Attention Sinks in Diffusion Language Models. [32] extends the study of attention sinks to DLMs, showing that attention sinks persist, but with different behavior: in DLMs, the positions of attention sinks tend to shift during the generation process as tokens are progressively unmasked. Moreover, these sinks can be masked without significant degradation. [52] addresses this moving-sink behavior by adding an additional sink token that is globally visible to all other tokens while attending only to itself. Such a token is shown to stabilize DLM inference.

Attention Sinks in Video Diffusion Transformers. [53] presents the first analysis of attention sinks in video DiTs, highlighting similarities and differences with LLMs. Notably, they find that these sinks are concentrated in the first frame, analogous to the <BOS> token in LLMs. [33, 54] consider an autoregressive approach to video generation, predicting multiple frames simultaneously. Similar to LLMs [30], they find that it is important to retain the first frame, which acts as an attention sink. [55] extends the idea of keeping the initial frame by proposing Deep Sink, which aims to stabilize global context during long rollouts. Note that video DiTs use attention sinks mainly to enable long-horizon AR sampling, rather than to study their effect on denoising performance.

Attention Sinks in Text-to-Image DiTs. For text-to-image diffusion, [56] highlights the special role of text tokens across different denoising steps, while [34] studies high-norm activations in pretrained text-to-image DiTs. However, these works do not fully characterize the nature or functional role of such tokens. Our work addresses this by systematically investigating high-norm tokens and connecting them to register tokens.

Outliers in Feature Dimensions. Another line of work studies outliers that emerge not across tokens, but within feature (channel) dimensions of learned representations [57, 7, 58, 59]. Initially studied in LLMs [57], this phenomenon was later analyzed in DiTs [58, 59]. In particular, [58] links massive activations to layer normalization, while [59] shows that manipulating them can improve fine-grained image details.

Register Tokens in Vision Transformers. Several works study the role and behavior of register tokens in ViTs [12, 13, 14, 15, 16, 17, 48]. [12] introduces register tokens to avoid sink artifacts in attention maps, improving ViT internal representations. Subsequent studies further analyze their functional role, showing that they can influence feature aggregation [14]. [13, 16] study post-hoc or self-distilled ways to add registers to pretrained ViTs without full retraining. [15] argue that register tokens alone do not fully explain or resolve all ViT artifacts. Recent large-scale ViTs also retain explicit outlier-handling mechanisms: DINOv3 adopts register tokens after comparing them with attention-bias and value-gating alternatives inspired by LLM outlier analyses [7].

To summarize, tokens with unusually large norms have been studied across different domains [29]. In this work, we extend this research direction to image diffusion transformers and show that they are particularly important for pixel-space models.

B Implementation Details

B.1 Analysis Implementation Details

In our implementation of pDiTs, we largely follow the JiT setup [24]. The model uses flow matching with x -prediction and the forward process $x_t = tx + (1 - t)\epsilon$, where $t = 1$ corresponds to clean data. We adopt the same diffusion backbone, but remove in-context conditioning and instead introduce register tokens implemented as trainable parameters without additional layers.

Snippet 1. RMSNorm Dual	Snippet 2. SwiGLU MLP Dual	Snippet 3. adaLN Dual
<pre># registers + patches # x: [B, n_reg + n_patch, h] # dual RMSNorm (x_reg, x_patch) = split(x) # separate normalization x_patch = RMSNorm(x_patch, w1, eps1) x_reg = RMSNorm(x_reg, w2, eps2) # merge streams x = concat(x_reg, x_patch)</pre>	<pre># shared hidden latent x1, x2 = chunk(Linear(x)) hidden = silu(x1) * x2 # split output projection (h_reg, h_patch) = split(hidden) y_reg = Linear(h_reg) y_patch = Linear(h_patch) # merge streams y = concat(y_reg, y_patch)</pre>	<pre># condition # c: [B, h] # shared modulation m = Linear(silu(c)) # dual branch params m_r = m + LoRA(c) (shift_reg, scale, gate) = split(m) (shift_reg, scale_reg, gate_reg) = split(m_r)</pre>

We train models of three sizes – B (131M), L (459M), and H (953M) – on ImageNet 256×256 . For the B and L models, we use a batch size of 1024, following JiT [24]. Due to limited computational resources, the H model is trained with a smaller batch size of 512. All other training and inference settings follow JiT [24].

For the latent-space models presented in Table 2, we follow their original setups [39, 21]. For RAE-XL, we use a smaller batch size (256 instead of 1024) due to computational constraints and train the model for 80 epochs. For SiTs, we use the same batch size as in the original implementation and train the models for 300 epochs. Register tokens are implemented in the same manner as in the pixel-space models.

B.2 Dual-Stream Implementation Details

In our analysis, we consider a parameter-efficient dual-branch architecture built on top of the JiT model with in-context conditioning, as it demonstrates better performance than pure register tokens. Through ablation studies, we find that the most critical components for effective separation are the RMSNorm, SwiGLU MLP, and adaLN layers. We present their implementations in Snippets 1, 2, and 3.

We consider models of two sizes, B and L, and train them on ImageNet at resolutions of 256 and 512. The proposed architecture introduces an additional parameter overhead of approximately 14%. We train the models using the same training and inference configuration as in JiT [24]. For both configurations, we use LoRA with rank 128 in AdaLN.

C Additional Analysis Results

C.1 Analysis on ImageNet

Outliers in DiTs. In the main text, we show that DiTs are free from the artifacts observed in ViTs. However, introducing register tokens leads to the emergence of high-norm tokens within the registers themselves. While the main analysis focuses on the small-scale pDiT-B/16 model at a single timestep ($t = 0.5$), here we present the corresponding results for additional timesteps, larger model variants, and latent-space counterparts.

First, Figure 9 shows that this effect consistently holds across different timesteps.

Second, Figure 10 shows that the observations made for pDiT-B/16 also hold for larger pixel-space variants, namely pDiT-L/16 and pDiT-H/16. Models without registers maintain relatively uniform patch-token norms across layers, without pronounced outliers. Once registers are introduced, however, large-norm tokens systematically emerge within the register tokens.

Second, we analyze the latent-space models SiT [21] and RAE [39] in terms of outlier behavior. Figure 11, 12 show that the same phenomenon also holds for latent-space diffusion models.

Improving Feature Map Quality. Next, we find that register tokens consistently reduce the feature norms of patch tokens. In Figure 13, we show this effect for larger pixel-space variants of pDiT. Interestingly, we do not observe the same behavior in SSL ViTs such as DINOv2, as shown in Figure 19.

	RAE-space pDiT backbone	VAE-space pDiT backbone	Pixel-space pDiT backbone
	<i>Base size</i>		
With registers	10.12	7.17	5.30
Without registers	9.40	7.20	7.39

Table 8: **Registers are more effective in pixel-space.** We compare the generation quality (FID) of models with and without register tokens across different training spaces (DINOv2, VAE, and pixel space) using the same pDiT backbone. Register tokens provide the largest improvements in pixel space, moderate gains in VAE space, and degrade performance in DINOv2 space (RAE).

Second, we show that register tokens improve feature quality across larger pDiT variants. Figure 14 reports the TV ratio for pDiT-L/16 and pDiT-H/16. In addition, Figure 15 analyzes the correlation decay slope [45], where lower values indicate stronger spatial organization. Both metrics show the same trend: register tokens improve internal representations at high noise levels, beginning at block 4, where the registers are introduced.

Effect of Register Injection Layer and Number of Register Tokens. Our analysis shows that, unlike ViTs where register tokens are effective from the first layer [12], pDiT-B/16 benefits primarily from their delayed introduction. For instance, introducing registers across all layers (0–11) results in performance similar to a model without registers.

Here, we provide a hypothesis for why this effect occurs. In Figure 16, we present linear probing results for register tokens introduced from layers 0 and 4. Importantly, we observe a notable difference between these two configurations. Specifically, models with registers introduced from the first layer produce substantially less informative register tokens. That is, we observe many tokens with moderate feature norms but very low probing accuracy. This suggests that these tokens serve neither as norm sinks nor as carriers of semantic information. Since we measure these results after the 5th block, we hypothesize that this poor signal from register tokens can negatively affect later layers and consequently degrade model performance.

We hypothesize that this poor register signal arises because, in the early layers of pDiTs, the model has not yet formed meaningful semantic structure. As a result, register tokens cannot capture diverse semantic information and instead propagate uninformative features.

Pixel-space versus Latent-space. In the main text, we show that register tokens provide substantially larger gains for pixel-space models. In Table 8, we further present results for additional backbones in RAE and VAE spaces and observe the same trend: performance degrades for RAE-based models, while VAE-space models show similar performance with and without registers. This suggests that the effect is not backbone-specific.

Next, we provide an explanation for this behavior through an analysis of token feature norms and intermediate representations across different model types. In Figures 17 and 18, we observe that pDiTs consistently exhibit the largest feature norms and the noisiest intermediate representations compared to latent-space counterparts. Specifically, Figure 17 shows that patch-token norms in pDiTs are substantially higher across all timesteps, while Figure 18 demonstrates that their intermediate features have significantly larger TV values.

These observations suggest that pixel-space diffusion produces substantially noisier intermediate features, which may explain why register tokens are especially beneficial in this setting.

C.2 Analysis on Text-to-Image Models

In addition to ImageNet-based DiTs, we consider large scale text-to-image approaches. We do not train these models with registers but consider pretrained open-sourced versions. Specifically, we analyze FLUX [46] and SD3.5 Large [42], which propagate textual information through an auxiliary token sequence appended to the image tokens. Importantly, this sequence does not directly participate in the diffusion loss, raising the possibility that it may partially serve a register-like role.

Method	200 epochs	600 epochs
pDiT-B/16 + PixelREPA	4.15	3.38
pDiT-B/16 (w/o registers) + PixelREPA	4.78	3.56
JiT-B/16 + PixelREPA + compact dual	3.68	3.23
JiT-B/16 + PixelREPA	4.00	3.40

Table 9: **REPA remains complementary to register-like tokens and further benefits from the proposed compact dual-stream design.** We evaluate pDiT models with and without register tokens using PixelREPA [60] on ImageNet 256×256 . Register-like tokens consistently improve performance, and combining them with the proposed compact dual-stream architecture further improves the results.

	Registers configuration			FID at Epoch		
	Size	Start	End	40	80	120
w/ reg.	32	4	11	37.7	9.59	6.45
	32	4	9	36.9	9.95	6.65
	32	0	11	59.7	19.3	11.9
	32	0	4	62.4	19.6	12.3
	16	4	11	40.4	10.2	6.80
	16	0	11	62.4	18.6	11.3
	4	4	11	46.3	12.8	8.37
	4	0	11	54.8	16.2	10.4
w/o reg.	—	—	—	60.6	18.4	11.1

Table 10: **Registers are effective only in deeper layers.** Unlike DINOv2, pDiT-B/16 benefits from registers only after the first 4 layers. Early-layer registers match the no-register baseline, while more registers improve performance.

For SD3.5 (Figure 20, left), we observe that high-norm outliers predominantly emerge within the text-token sequence, while image-token norms remain comparatively uniform. This behavior closely resembles the role of register tokens in ImageNet-based DiTs, suggesting that auxiliary text tokens may implicitly act as repositories for high-norm representations.

Interestingly, for FLUX (Figure 20, right), we observe not only outliers in text tokens but also several high-norm image tokens. We hypothesize that this difference stems from architectural design choices: FLUX employs dual-stream layers only in the early stages of the network, whereas SD3.5 maintains dual-stream processing throughout all layers.

D Additional Experimental Results

In Table 9, we evaluate whether register-like tokens remain beneficial when combined with representation alignment [44]. We adopt the recent REPA adaptation [60], which was specifically proposed for JiT-based architectures. We observe that register tokens consistently improve the performance of REPA-enhanced models. In addition, our compact dual-stream architecture remains effective with REPA.

In addition, we ablate different register-token configurations in Table 10, varying both the number of registers and the transformer blocks in which they are enabled. The results show that delayed introduction is crucial: configurations that activate registers only in deeper layers (4–11) consistently outperform both the no-register baseline and configurations where registers are introduced from the first layer (0–11). We also observe that increasing the number of registers improves performance, with 32 registers yielding the best results. Finally, comparing the 4–11 and 4–9 settings suggests that the latest layers contribute relatively little to the effectiveness of registers.

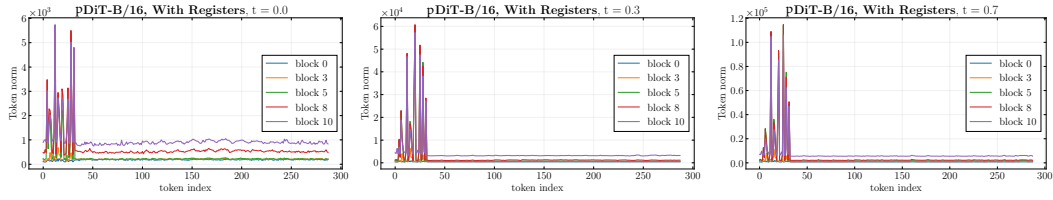


Figure 9: **High-norm outliers consistently emerge within register tokens across timesteps.** We visualize token-wise feature norms of pDiT-B/16 with registers for $t = 0.0, 0.3,$ and $0.7,$ and observe the same behavior in all cases.

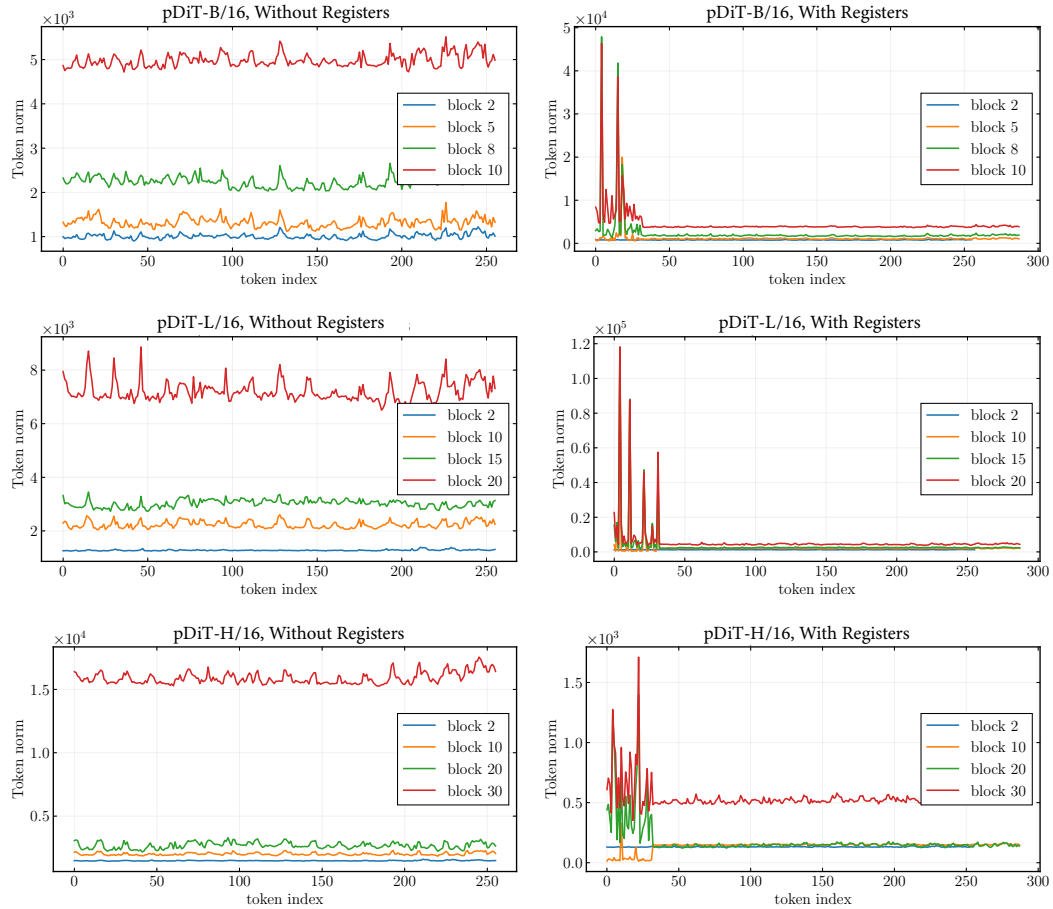


Figure 10: **Token-wise feature norms for pDiTs of varying scales on ImageNet $256 \times 256,$ with and without registers.** Without registers, patch-token norms remain uniform across scales. Introducing registers leads to the emergence of high-norm outliers within the register tokens.

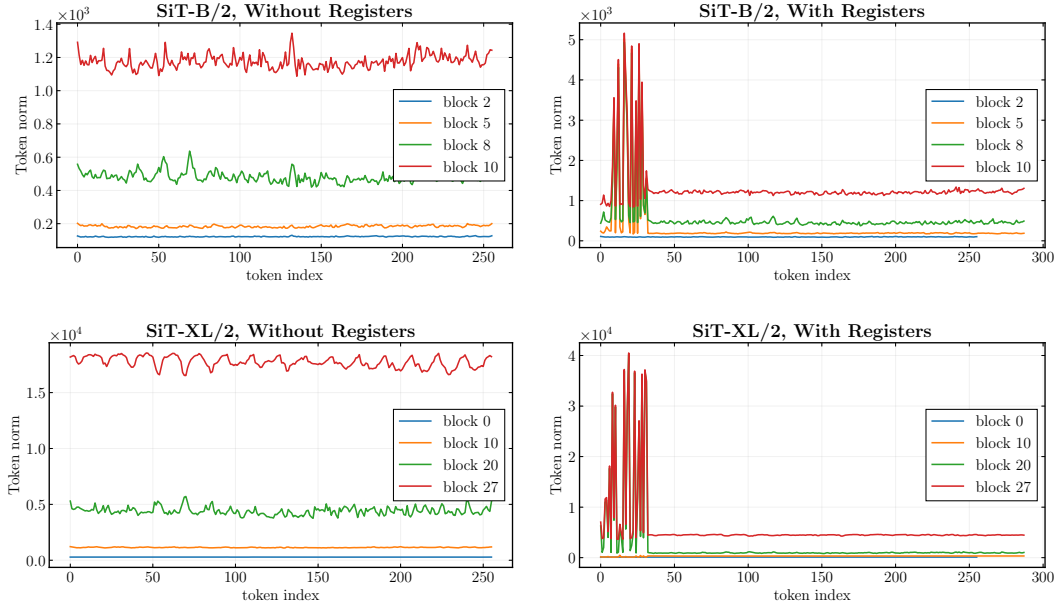


Figure 11: Token-wise feature norms for VAE-space SiTs of varying scales on ImageNet 256×256 , with and without registers. SiTs without registers exhibit uniform patch-token norms across scales, while adding registers produces high-norm register tokens.

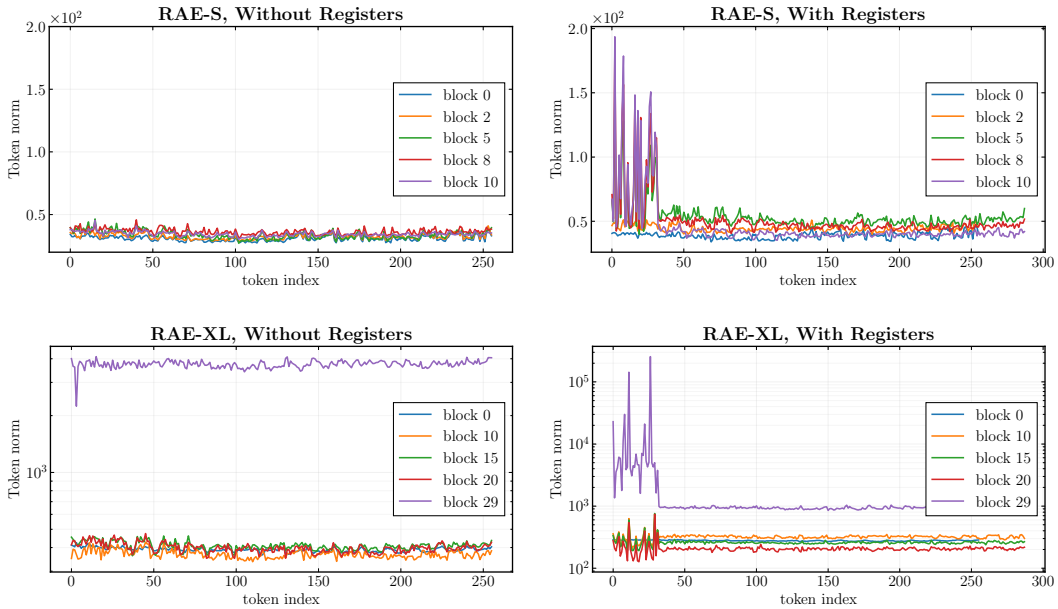


Figure 12: Token-wise feature norms for DINOv2-space RAEs of varying scales on ImageNet 256×256 , with and without registers. RAEs without registers exhibit uniform patch-token norms across scales, while adding registers produces high-norm register tokens.

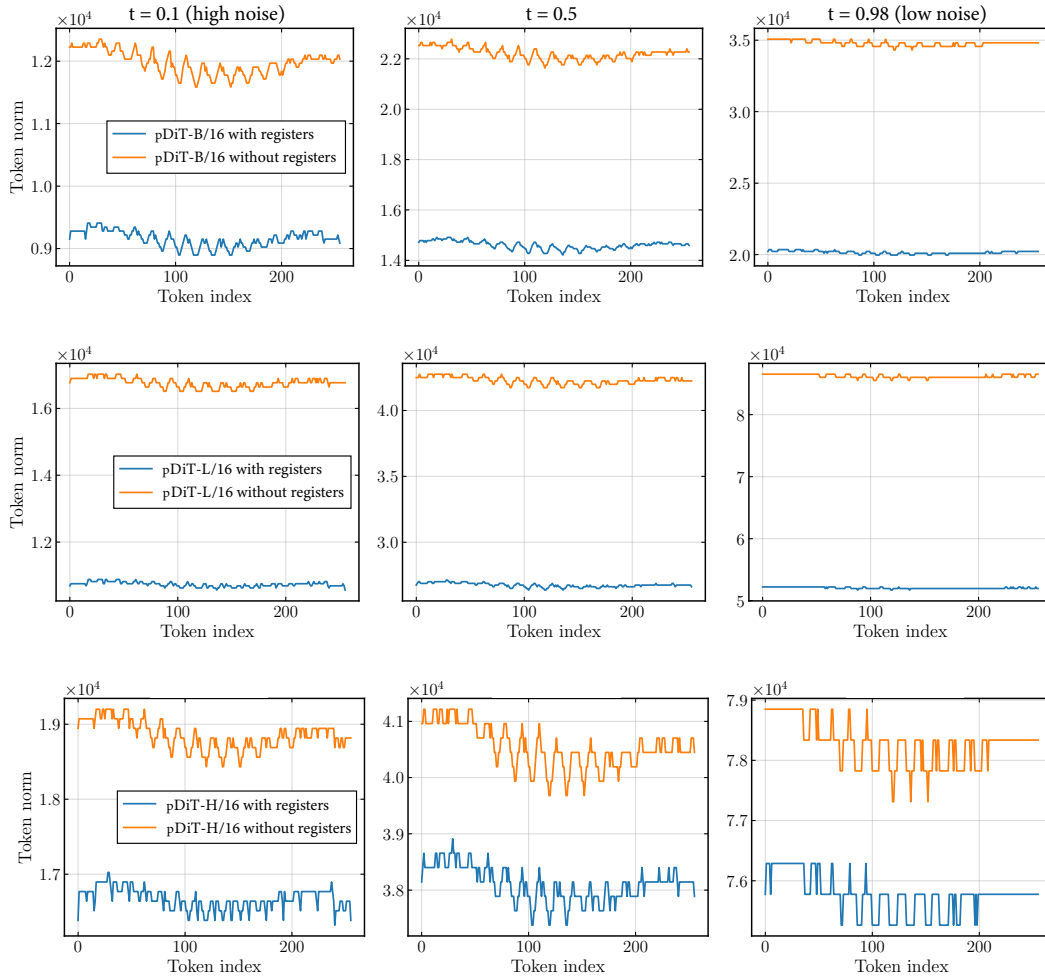


Figure 13: **Register tokens consistently reduce feature norms across patch tokens.** We measure feature norms for image tokens only (excluding register tokens) at three diffusion timesteps for pDiT models of different scales, and observe a consistent reduction in feature norms across nearly all tokens when register tokens are used.

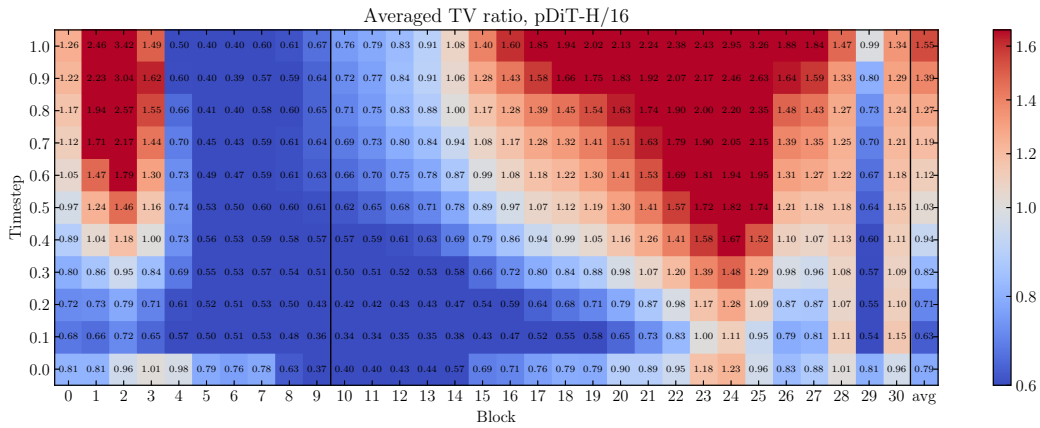
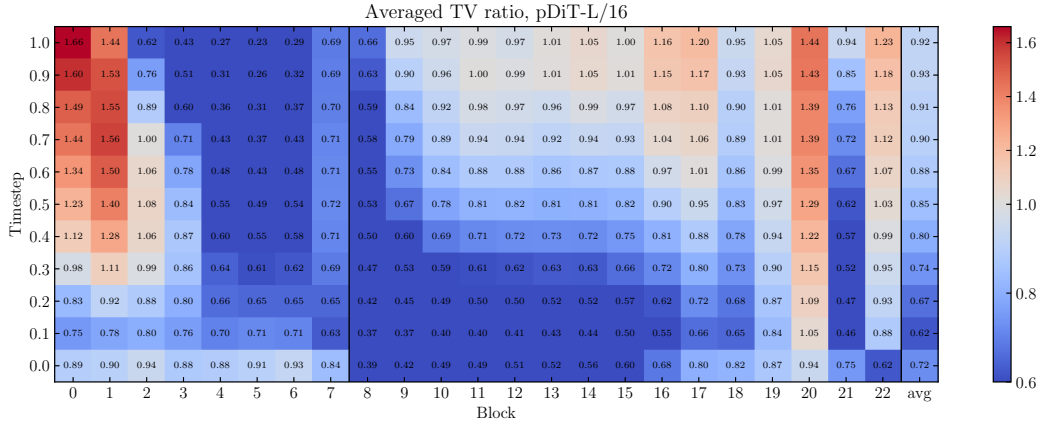


Figure 14: **Register tokens make intermediate representations cleaner by reducing noise.** We compute the Total Variation of intermediate features for models with and without register tokens. We report the ratio (with registers / without registers), where lower values indicate that models with registers produce smoother feature representations. We find that register tokens improve feature smoothness at high noise levels ($t \in [0, 0.2]$) for both pDiT-L/16 (top) and pDiT-H/16 (bottom) models.

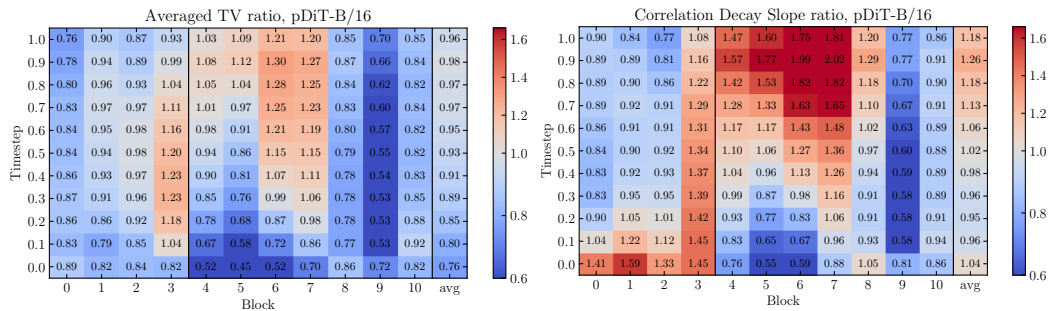


Figure 15: **Registers improve spatial organization at high noise levels.** In addition to the TV ratio (left), we also analyze the correlation decay slope [45] (right), where lower values indicate stronger spatial organization. Both metrics show the same trend: register tokens improve internal representations at high noise levels, starting from block 4, where the registers are introduced.

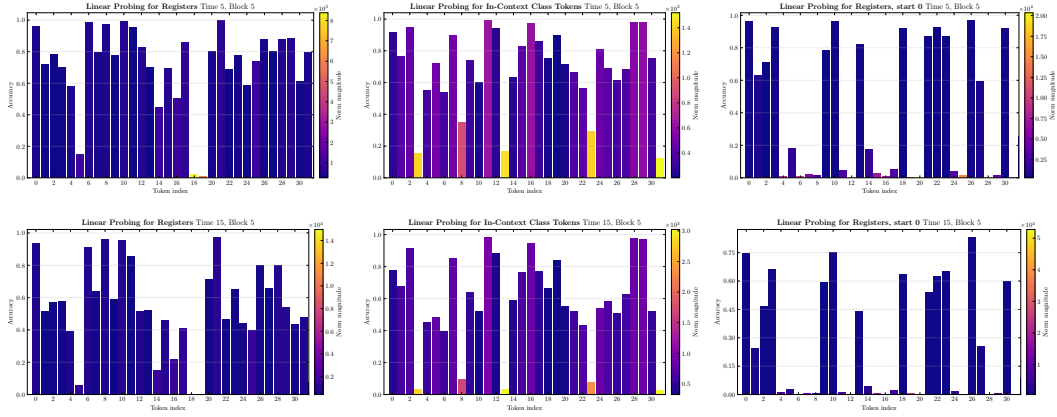


Figure 16: **Linear probing of register tokens under different configurations.** (Left) Standard register tokens introduced from the 4th layer; (Middle) Register tokens used as in-context class embeddings introduced from the 4th layer; (Right) Standard register tokens introduced from the 0th layer. Across different timesteps, we find that introducing registers from the earliest layers produces substantially less informative register tokens. In particular, we observe more low-norm (non-sink) tokens with poor linear probing accuracy.

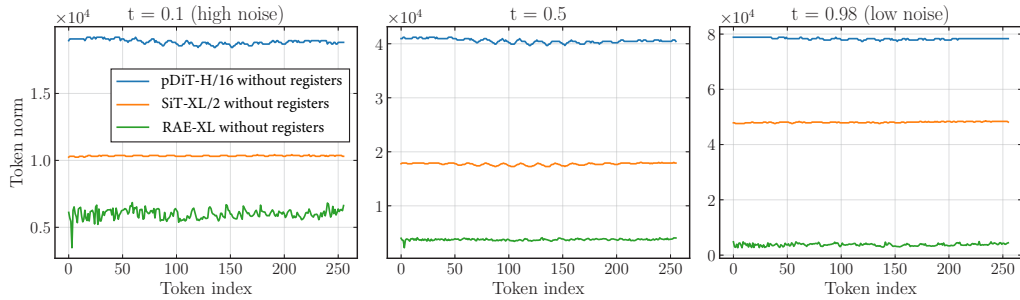


Figure 17: **Pixel-space pDiTs have the highest feature norms across all tokens for different timesteps compared to latent-space counterparts.** We compare token-wise feature-map norms for pDiT, SiT, and RAE models, all without register tokens.

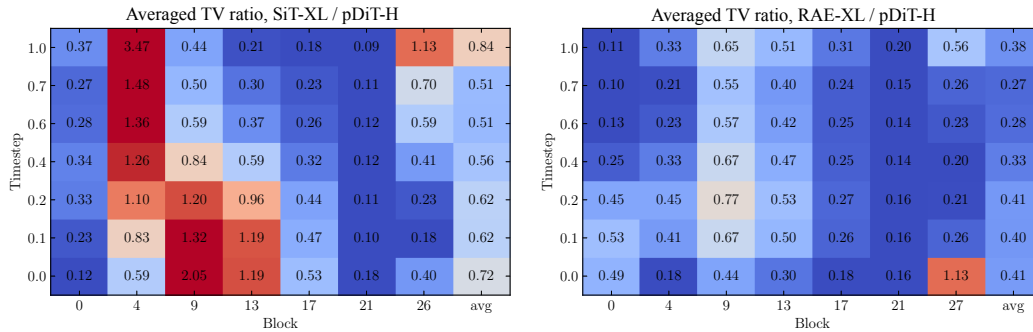


Figure 18: **Pixel-space pDiTs exhibit substantially higher Total Variation (TV) values than latent-space counterparts.** We compare the TV ratio of intermediate feature maps across timesteps and transformer blocks for pixel-space pDiTs (pDiT-H) and latent-space models (SiT-XL and RAE-XL) without registers. Pixel-space pDiTs consistently produce noisier intermediate representations.

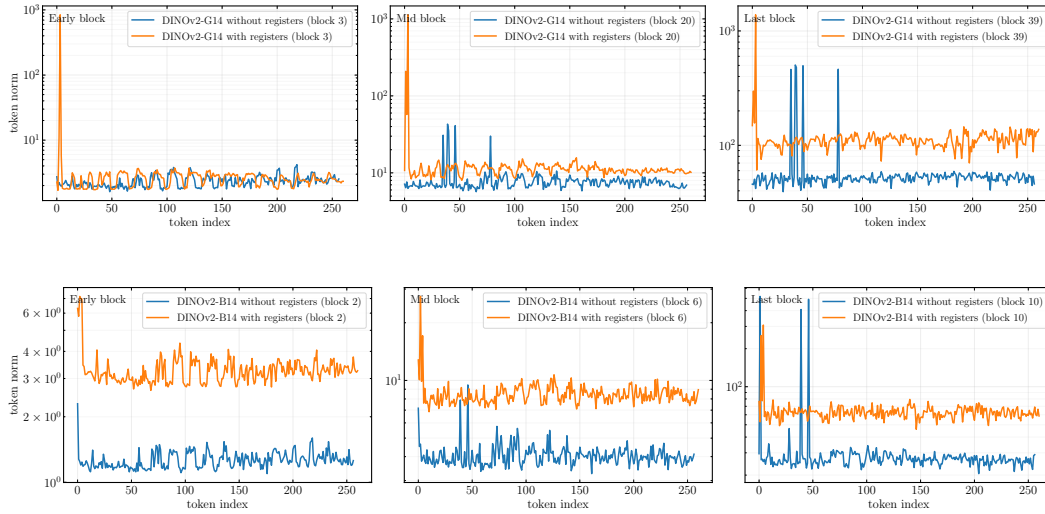


Figure 19: For SSL ViTs such as DINOv2, register tokens do not reduce patch-token feature norms, unlike in DiTs. We measure feature norms across all tokens for different blocks and model sizes of DINOv2, and observe that register tokens do not consistently reduce feature norms of patch tokens.

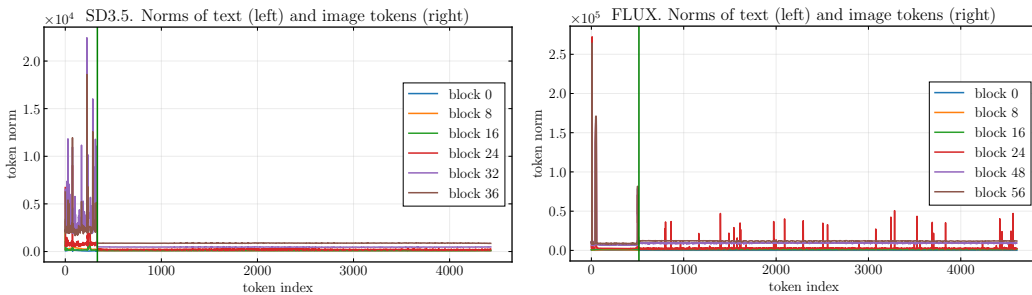


Figure 20: Text sequences in text-to-image diffusion models exhibit behavior similar to register tokens in ImageNet-based DiTs: some tokens become high-norm outliers and potentially act as registers. We measure token-wise feature norms in SD3.5 (left) and FLUX (right) for both text and image tokens. We observe that the outliers primarily emerge within the text sequence.